Estimation of the maximum friction coefficient for a passenger vehicle using the instantaneous cornering stiffness

Lukas Haffner, Martin Kozek, Jingxin Shi, and H. Peter Jörgl

Abstract— The estimation of the maximum lateral coefficient of friction of a passenger vehicle between tire and road is presented in this paper. This is achieved by utilizing the instantaneous cornering stiffness, which is defined as the slope of the nonlinear curve of the lateral friction coefficient at the instantaneous tire slip angle. The maximum lateral coefficient of friction is necessary for integrated global cassis control (IGCC) especially for the estimation of the lateral velocity of the vehicle. The advantage of this method is the low computational effort and the independence of tire or road conditions. Two methods for estimation of the instantaneous cornering stiffness and the maximum coefficient of friction in real time and a method for offline estimation used as a reference are described and validated using measured data of a passenger vehicle.

Fig. 1. Lateral tire model presenting the instantaneous cornering stiffness $C_\alpha(\alpha)$

I. INTRODUCTION

For IGCC it is necessary to have precise information about vehicle states and the tire-road condition. A main problem is to detect when the tire force reaches its maximum and the tires start to skid. This may result in a unstable driving situation. Many works have already been carried out on the slip based estimation of the maximum friction coefficient μ_{max} between tire and road. The longitudinal slip λ and the slip angle α are used for longitudinal and lateral dynamics, respectively. In the following publications a defined slope is used to identify μ_{max} for longitudinal and lateral considerations:

In [1] the slip slope k is defined as the slope of the μ_x-λ-curve at $\mu_x = 0$. The information of the slip slope and the variance of the slip signal leads to a defined road condition including a specific $\mu_{x,max}$. With this method four different road surfaces can be classified. In [2] the same assumption is made distinguishing between dry and wet asphalt only by estimating the slip slope. In [3] the extended braking stiffness XBS is defined as the slope of the F_x-λ-curve at any λ with F_x being the longitudinal force of the tire. The XBS is estimated by the power spectrum density of the angular velocities of the wheels.

The cornering stiffness c_0 is estimated in [4] to be used in active steering. c_0 is defined as the slope of the F_y-α-curve at $\alpha = 0$. In [5] the cornering stiffness C_α is estimated using the same definition like [4].

This paper concentrates on lateral dynamics including lateral

L. Haffner, M. Kozek, and H. P. Jörgl are with the Institute of Mechanic and Mechatronic, Division of Control and Process Automation, Vienna University of Technology, A-1040 Vienna, Austria

`lukas.haffner@tuwien.ac.at`
`martin.kozek@tuwien.ac.at`

J. Shi is with TTTech Germany GmbH, D-85276 Hettenshausen-Reisgang, Germany
`jingxin.shi@tttech.de`
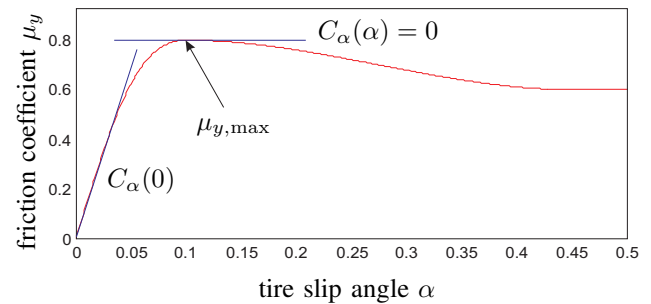
tire forces and tire slip angles. In contrast to [4] and [5] the instantaneous cornering stiffness $C_\alpha(\alpha)$ is defined as first derivative of the μ_y-α-curve similar to the definition in [3] for longitudinal dynamics. Thus it is not constant for static road conditions, but changes regarding the slope of the μ_y-α-curve.

For $C_\alpha(\alpha) = 0$, the maximum lateral coefficient of friction $\mu_{y,max}$ is reached. Hence, the vehicle state has to pass the non-monotone part of the lateral tire characteristics in order to detect $\mu_{y,max}$ as shown in Fig. 1 where $C_\alpha(\alpha)$ becomes zero or negative. An actual vehicle in such a driving situation will become unstable, and therefore the estimation of $\mu_{y,max}$ is essential for IGCC.

The proposed concept of instantaneous cornering stiffness estimation is therefore capable of not only detecting $\mu_{y,max}$, but also of estimating the instantaneous driving conditions. The remainder of the paper is organized as follows: In II a vehicle model and the used variables are defined, in III three estimation methods for $C_\alpha(\alpha)$ are presented, which is consequently utilized as an input to the $\mu_{y,max}$-estimation, in IV experimental results show the performance of these methods, and in V conclusions and future works are shown.

II. VEHICLE MODEL

The single-track model of Fig. 2 is used for further considerations with v_{CoG}, a_x, a_y, F_y, v, α, l, $\dot{\psi}$, δ and β being the velocity of the center of gravity, the longitudinal and lateral acceleration, the lateral force, the velocity of the tire, the tire slip angle, the distance from center of gravity to the tire, the yaw rate, the steering angle, and the sideslip angle of the vehicle, respectively. The indices F and R relate to the front and rear tire of the vehicle, respectively. The road inclination and superelevation are not taken into account. However, there exists literature where the problem of vehicle
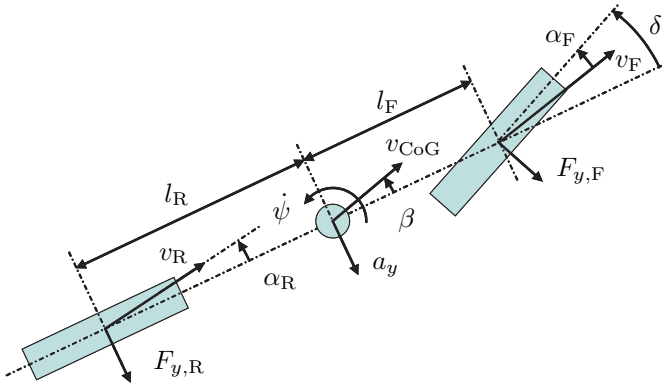
Fig. 2. Single-track model for vehicle lateral dynamics

state estimation in the presence of these road characteristics is treated extensively, e.g. [6].

The lateral and vertical tire forces F_y and F_z can be written as

$$F_{y,\mathrm{F}} = \frac{ma_y l_{\mathrm{R}} - J_z \ddot{\psi}}{(l_{\mathrm{F}} + l_{\mathrm{R}})cos\delta}, \tag{1}$$

$$F_{y,\mathrm{R}} = \frac{ma_y l_{\mathrm{F}} + J_z \ddot{\psi}}{l_{\mathrm{F}} + l_{\mathrm{R}}},$$

$$F_{z,\mathrm{F}} = \frac{m(gl_{\mathrm{F}} - a_x h)}{l_{\mathrm{F}} + l_{\mathrm{R}}}, \text{ and} \tag{2}$$

$$F_{z,\mathrm{R}} = \frac{m(gl_{\mathrm{R}} + a_x h)}{l_{\mathrm{F}} + l_{\mathrm{R}}}$$

with m, J_z and g being the vehicle mass, the moment of inertia and the gravitatonal constant. The front and rear lateral coefficient of friction read:

$$\mu_{y,\mathrm{F}} = \frac{F_{y,\mathrm{F}}}{F_{z,\mathrm{F}}} \tag{3}$$

$$\mu_{y,\mathrm{R}} = \frac{F_{y,\mathrm{R}}}{F_{z,\mathrm{R}}}$$

μ_y is a nonlinear function depending on the tire slip angle, the vehicle vehicle velocity, the tire and road condition and other parameters. The slip angles of the front and rear tires can be calculated with the following widely used approximation:

$$\alpha_{\mathrm{F}} = \delta - \beta - \frac{\dot{\psi} l_{\mathrm{F}}}{v_{\mathrm{CoG}}} \tag{4}$$

$$\alpha_{\mathrm{R}} = -\beta + \frac{\dot{\psi} l_{\mathrm{R}}}{v_{\mathrm{CoG}}}$$

Using the relations (1) to (4) the lateral vehicle dynamics can be computed for all driving situations. Since not all necessary variables are measured online, a combination of parameter estimation and observers becomes necessary (see Fig. 3). In order to reconstruct correct tire slip angles α_{F} and α_{R} in all driving conditions the cornering stiffness is of crucial importance.

III. ESTIMATION OF THE INSTANTANEOUS CORNERING STIFFNESS AND THE FRICTION COEFFICIENT

A. Basic Considerations
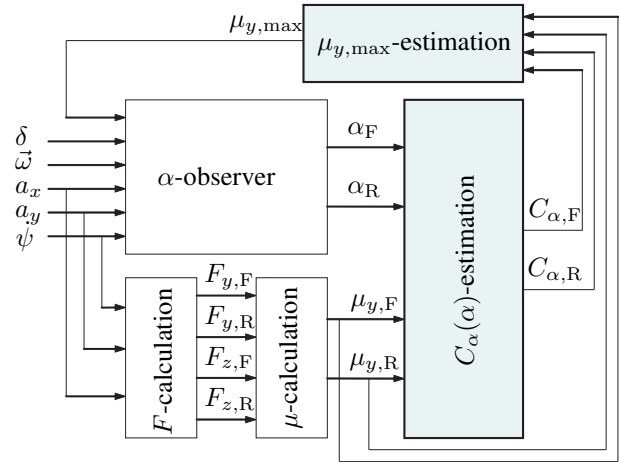
Fig. 3. Schematic of vehicle state estimation

For the estimation of the instantaneous cornering stiffness $C_\alpha(\alpha)$ the inputs μ_y and α are required. μ_y can be calculated with (1), (2) and (3) as a_x, a_y and $\dot{\psi}$ are measured in modern passenger vehicles. α has to be either measured or estimated by an observer. The measurement of α can be done indirectly by velocity sensors in longitudinal and lateral direction and with (4). Velocity sensors are expensive and not feasible in mass production. Alternatively, an α-observer uses a_x, a_y, δ, $\dot{\psi}$ and the four angular velocities of the wheels $\vec{\omega}$ as inputs. An extended Kalman filter as in [7] is used as well as nonlinear observer presented by [8] and [9]. The instantaneous cornering stiffness $C_\alpha(\alpha)$ indicates when $\mu_{y,\mathrm{max}}$ is reached, which is necessary for vehicle control. As additional input $\mu_{y,\mathrm{max}}$ can be used in the α-observer as shown in Fig. 3. As discussed in [11], another potential issue is the stability/convergence analysis in feeding back $\mu_{y,\mathrm{max}}$. Although not addressed in this paper, the problem of the stability/convergence of the overall state estimation (Fig. 3) has to be investigated in future works. For IGCC the instantaneous cornering stiffness has to be estimated in real-time. Therefore the algorithm has to work with limited computational effort and only utilizing present and past data. Two methods are presented for online estimation of $C_\alpha(\alpha)$:

- Least Squares Online Estimation (III-C)
- Weighted Recursive Least Squares Online Estimation (III-D)

The offline estimation (III-B) is used as a reference to the online methods.

B. Offline Estimation

For the offline estimation the whole data set can be used, even the values of future vehicle states. Thus it is possible to fit a tire model to the μ_y-α-data set. Similar to the tire

model presented in [10] the following more flexible structure is used:

$$\mu_y = \frac{a\alpha^2 + b\alpha}{c\alpha^2 + d\alpha + 1} \quad (5)$$

The four parameters of the tire model have to be optimized to get a curve fitting regarding to total least squares (TLS) [12]. Because of different noise levels of μ_y- and α-data, a normalization has to be done before executing the algorithm. The data has to be filtered with a high pass filter in order to get the noise signal for each data. The standard deviation σ of the noise signals is now used for the normalized coefficient of friction μ_y^{n}:

$$\mu_y^{\mathrm{n}} = \mu_y \frac{\sigma_\alpha}{\sigma_{\mu_y}} \quad (6)$$

The n data points $[P_1^{\mathrm{d}}, P_2^{\mathrm{d}}, ..., P_i^{\mathrm{d}}, ..., P_j^{\mathrm{d}}, ..., P_n^{\mathrm{d}}]$ relate
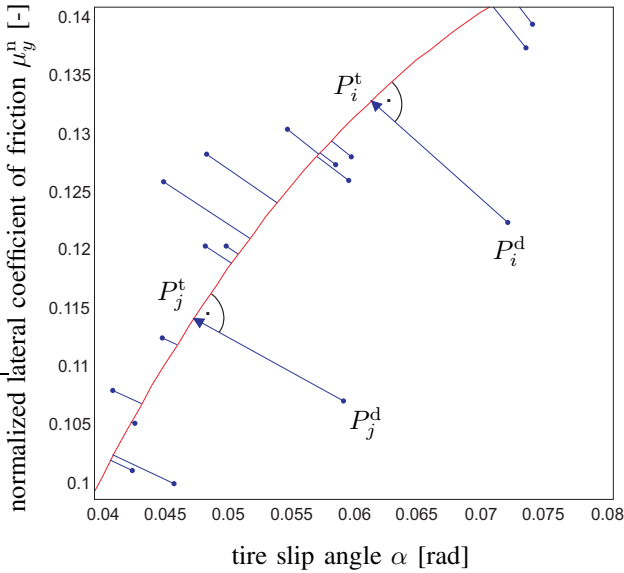
Fig. 4.   Projection of the data points orthogonally on the fitted tire model

to the n points $[P_1^{\mathrm{t}}, P_2^{\mathrm{t}}, ..., P_i^{\mathrm{t}}, ..., P_j^{\mathrm{t}}, ..., P_n^{\mathrm{t}}]$ on the tire model so that the line $\overline{P_i^{\mathrm{d}} P_i^{\mathrm{t}}}$ is orthogonal to the tire model respectively to its slope at P_i^{t} as shown in Fig. 4. The parameter vector is optimized iterative using a constant step size. For all the permutations of the parameter vector the criterion V of the summed squared orthogonal distances

$$V = \sum_{i=1}^{n} \overline{P_i^{\mathrm{d}} P_i^{\mathrm{t}}}^2 \quad (7)$$

has to be calculated. The parameter vector with minimum V becomes the new vector for the next iteration step. So the parameter vector converges to a vector fitting the tire model to the data points. Considering the definition of

$$P_i^{\mathrm{d}} = [\alpha_i^{\mathrm{d}}, \mu_{y,i}^{\mathrm{d}}] \quad \text{and} \quad (8)$$
$$P_i^{\mathrm{t}} = [\alpha_i^{\mathrm{t}}, \mu_{y,i}^{\mathrm{t}}] \quad (9)$$

the instantaneous cornering stiffness $C_{\alpha,i}$ can now be written as:

$$C_{\alpha,i}^{\mathrm{ref}} = C_\alpha(\alpha_i^{\mathrm{d}}) = \left. \frac{d\mu_y}{d\alpha} \right|_{\alpha=\alpha_i^{\mathrm{t}}} \quad (10)$$

This method needs a lot of computational effort. On the one hand, the fitting of the tire model to the measured data needs many calculation steps. On the other hand, the calculation of the related data points of the tire model has to be performed for each data point. However, this method is reasonable as a reference to benchmark the methods for online estimation.

C. Online Estimation with LS

For this method a regression line is calculated for a defined data window of the length l. The instantaneous cornering stiffness $C_{\alpha,i}$ representing the i-th data point can be written as slope of above mentioned regression line

$$C_{\alpha,i}^{ls} = \frac{\sum_{k=i-l}^{i} (\alpha_k - \bar{\alpha}_i)(\mu_{y,k} - \bar{\mu}_{y,i})}{\sum_{k=i-l}^{i} (\alpha_k - \bar{\alpha}_i)^2} \quad (11)$$

with $\bar{\alpha}_i$ and $\bar{\mu}_{y,i}$ being the mean value of the data set $[\alpha_{i-l}, ..., \alpha_i]$ and $[\mu_{y,i-l}, ..., \mu_{y,i}]$. It is necessary to use a variable window length to have a satisfying performance at any driving situation. The window length l is chosen minimal fulfilling the condition

$$max([\alpha_{i-l}, ..., \alpha_i]) - min([\alpha_{i-l}, ..., \alpha_i]) \geq \Delta\alpha_{\mathrm{min}} \quad (12)$$

with $\Delta\alpha_{\mathrm{min}}$ being constant. If $\Delta\alpha_{\mathrm{min}}$ is chosen large, the estimation will be slow especially at large values of $\frac{d\alpha}{dt}$. Choosing a small value leads to a poor estimation being very dependent on noise. For further consideration $\Delta\alpha_{\mathrm{min}}$ should be optimized by fulfilling an optimization criterion.

D. Online Estimation with WRLS

In this section the regression line is calculated with the WRLS-algorithm. The vector Θ includes the two parameters of the regression line and is calculated recursively with $x_i = [\alpha_i, 1]$ and $y_i = \mu_{y,i}$, the forgetting factor λ, and the covariance of the error P:

$$\gamma = \frac{P_{i-1} x_i}{x_i^T P_{i-1} + \lambda} \quad (13)$$
$$P_i = \frac{1}{\lambda}(1 - \gamma x_i^T) P_{i-1} \quad (14)$$
$$\Theta_{i+1} = \Theta_i + \gamma(y - x_i^T \Theta_i) \quad (15)$$

$C_{\alpha,i}^{wrls}$ is given by the first entry of Θ_i. Like in [13] a variable forgetting factor is used. Similar to the window length l in III-C the data points of the past are weighted by λ. λ is assumed as proportional to l with a lower and upper saturation:

$$\begin{aligned} \lambda = \lambda_{\mathrm{min}} & \quad \text{for} \quad l \leq l_{\mathrm{min}} \\ \lambda = \lambda_{\mathrm{min}} + \frac{l - l_{\mathrm{min}}}{l_{\mathrm{max}} - l_{\mathrm{min}}} & \quad \text{for} \quad l_{\mathrm{min}} < l < l_{\mathrm{max}} \\ \lambda = \lambda_{\mathrm{max}} & \quad \text{for} \quad l \geq l_{\mathrm{max}} \end{aligned} \quad (16)$$

The constraints λ_{max} and λ_{min} have to be chosen to have an accurate estimation at $l \geq l_{\mathrm{max}}$ and a fast performance at

$l \leq l_{\min}$. Together with $\Delta\alpha_{\min}$ used for the calculation of l in (12) there are 5 free parameters for the optimization of λ. These could be chosen by minimizing a criterion in order to get optimal performance.

E. Estimation of $\mu_{y,\max}$

As shown in Fig. 1 the maximum coefficient of friction $\mu_{y,\max}$ is reached when $C_\alpha(\alpha) = 0$. Because of measurement noise this condition has to be relaxed in order to get a robust $\mu_{y,\max}$-detection (see Fig. 3):

$$C_\alpha(\alpha_i) < C_{\alpha,\mathrm{crit}} \quad \Longleftrightarrow \quad \mu_{y,\max,i} \equiv \mu_{y,i} \quad (17)$$

$$C_\alpha(\alpha_i) \geq C_{\alpha,\mathrm{crit}} \quad \Longleftrightarrow \quad \mu_{y,\max,i} = 1 \quad (18)$$

The constant $C_{\alpha,\mathrm{crit}}$ has to be chosen such that for given vehicle data a robust detection results. As an input in an α-observer, $\mu_{y,\max}$ is only needed in the nonlinear region of the tire model. In the linear region the cornering stiffness $C_\alpha(0)$ is essential. Therefore $\mu_{y,\max}$ is assumed to be 1 according to (18), as long as data are only available for the linear region of the tire model.

IV. EXPERIMENTAL RESULTS

The measurement was done with a modern passenger vehicle having attached velocity sensors. Thus it is possible to calculate α with (4). In the first experiment the vehicle was doing a circle movement on wet road. With increasing speed and steering angle the vehicle starts to skid, reaching a velocity of 20m/s. After reducing velocity and steering angle, α decreases abruptly reaching the monotone part of the tire model. In Fig. 5 the reference $C_\alpha^{\mathrm{ref}}(\alpha)$ starts at high level and reaches the low level at about $t = 6$s, where $C_\alpha(\alpha)$ becomes zero or even negative. At $t = 12$s $C_\alpha(\alpha)$ is changing rapidly back to high level.
Both the LS- and WRLS-estimation do not reach the value of the reference algorithm at high level, because of the effect of the noise of α. However, the high and low level can be distinguished in their value. The LS-estimation follows the reference-curve rapidly at changes, but it is varying strongly at low level due to small window length l shown in Fig. 6. The WRLS-algorithm causes a filtering, making noise of the signal of $C_\alpha^{\mathrm{wrls}}(\alpha)$ very small.

Even though the forgetting factor λ is chosen variable as shown in Fig. 7 the WRLS-estimation is not as fast as the LS-estimation at the change of $C_\alpha(\alpha)$ high to low level. It is hard to chose the parameters of the variable forgetting factor in (16) so that the estimator works well in every part. That is the reason of errors in the constant high level area at 0s $< t < 6$s and 13s $< t < 15$s. In the second experiment the vehicle was absolving a slalom course on dry road at a velocity of 20m/s. In Fig. 8 the LS- and WRLS-estimation follow the reference only with a small time delay and the low and high level areas can be separated. Because of the fast change of α in slalom maneuvers l and λ are very small. The time delay is not caused by the computational effort of the estimation, but because of the noisy data and the usage of
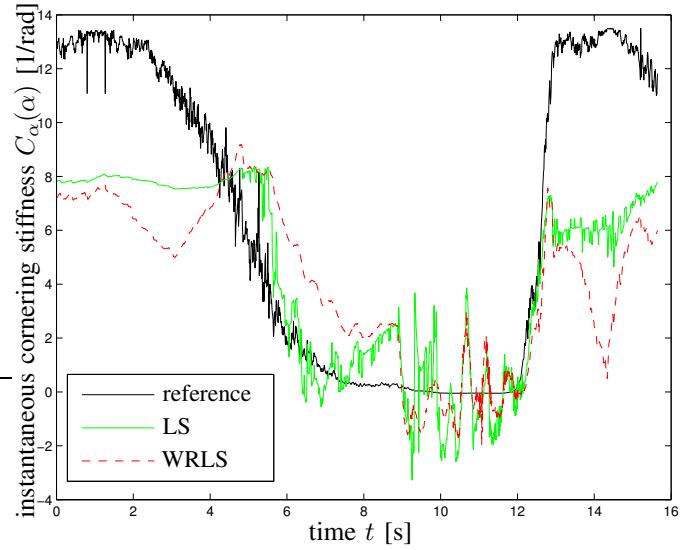
Fig. 5. Validation of the $C_\alpha^{\mathrm{ls}}(\alpha)$- and $C_\alpha^{\mathrm{wrls}}(\alpha)$-estimation method at a circle movement on wet road
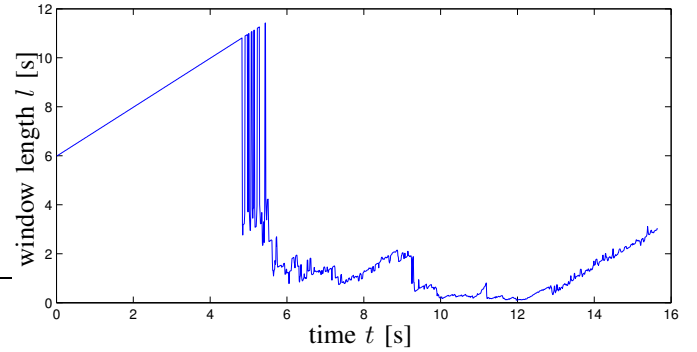
Fig. 6. Window length l referring to the LS-estimation in Fig. 5

only the past data. However, the LS-estimation is sufficiently fast and accurate for the use in vehicle control.

In Fig. 9 the validation of the $\mu_{y,\max}$-estimation is shown. The vehicle is moving along four different surfaces with different values of $\mu_{y,\max}$:

dry asphalt	$\mu_{y,\max} = 0.85$	$0s < t \leq 12s$
wet asphalt	$\mu_{y,\max} = 0.75$	$12s < t \leq 24s$
snow	$\mu_{y,\max} = 0.25$	$24s < t \leq 36s$
ice	$\mu_{y,\max} = 0.05$	$36s < t \leq 60s$

On dry and wet asphalt the vehicle is accelerating to 70km/h with increasing steering angle. On snow the vehicle is doing a slalom maneuver with 40km/h. On the icy surface the vehicle is doing a cornering maneuver with 25km/h reaching a front sideslip angle of 0.15rad. According to (18) $\mu_{y,\max}$ is set to the value 1 when the vehicle is moving in the linear region of the tire model, which is defined by $C_\alpha(\alpha) \geq C_{\alpha,\mathrm{crit}}$, where $C_{\alpha,\mathrm{crit}} = 1$ was found to deliver good results. The reference algorithm can clearly distinguish between the surfaces and detect the correct value of $\mu_{y,\max}$. The LS-Estimation can not distinguish between dry and wet asphalt,
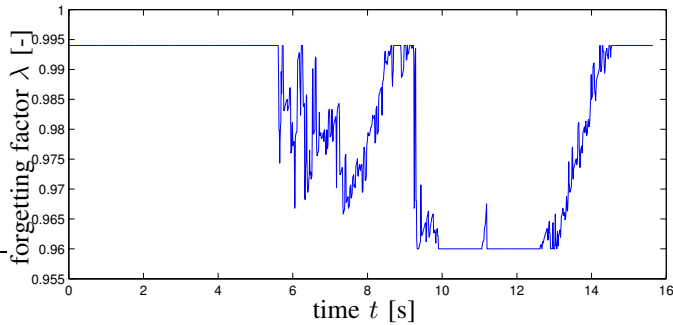
Fig. 7. Forgetting factor λ referring to the WRLS-estimation in Fig. 5
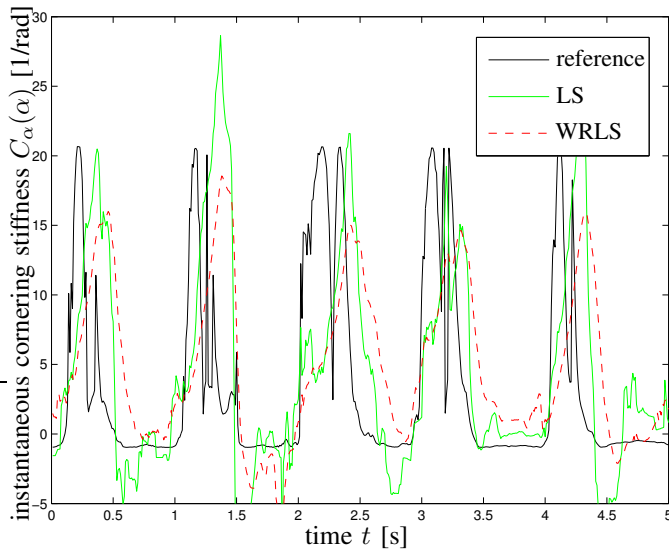
Fig. 8. Validation of the $C_\alpha^{ls}(\alpha)$- and $C_\alpha^{wrls}(\alpha)$-estimation method at a slalom movement on dry road
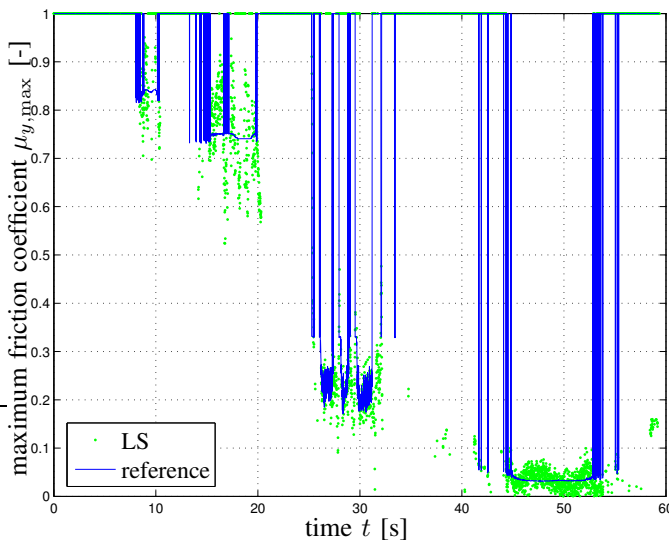
Fig. 9. Validation of the $\mu_{y,\max}$-Estimation on four different surfaces

but shows an accurate and fast behavior on snow and ice. Values of $\mu_{y,\max} = 1$ for short durations on wet asphalt and snow are caused by short stretches of straight driving. Under these driving conditions no information on the current value of $\mu_{y,\max}$ is available and an estimation scheme for the maximum longitudinal friction coefficient $\mu_{x,\max}$ would have to be implemented. Because of the higher performance of the LS-Estimation, the WRLS-Estimation is not shown here.

V. CONCLUSIONS AND FUTURE WORKS

A. Conclusions

The method described in III-B works well for the offline estimation of the instantaneous cornering stiffness. The LS-estimation is very flexible due to the variable window length l and has a satisfying performance at both constant and changing tire slip angle, using only one parameter for the calculation of l. The forgetting factor of the WRLS-algorithm can be tuned by 5 parameters, but the structure of the variable forgetting factor is not flexible enough to satisfy under all driving conditions. Therefore, the LS-estimation of the instantaneous cornering stiffness was used for the $\mu_{y,\max}$-estimation and leads to accurate results.

B. Future Works

A suitable criterion can be incorporated into the computation of the variable window length l of the LS-estimation and the optimal parameters of the forgetting factor λ of the WRLS-estimation. Finding other structures of λ could lead to a better performance as well. Since the output of the $\mu_{y,\max}$-estimation presented in this paper is still affected by noise, an improvement can be expected by implementing a suitable filter.

VI. ACKNOWLEDGMENTS

REFERENCES

[1] F. Gustafsson, "Slip-based Tire-Road Friction Estimation", *Automatica*, vol. 33 no. 6, 1997, pp 1087-1099.
[2] C. Lee, K. Hedrick, and K. Yi, "Real-Time Slip-Based Estimation of Maximum TireRoad Friction Coefficient", *IEEE/ASME Transactions on Mechatronics*, vol. 9, no. 2, 2004
[3] T. Umeno, "Estimation of Tire-Road Friction by Tire Rotational Vibration Model", *R&D Review of Toyota CRDL*, vol. 37 No. 3, 2002
[4] W. Sienel, "Estimation of the Tire Cornering Stiffness and its Application to Active Car Steering", *Proceedings of the 36th Conference on Decision and Control*, 1997, pp 4744-4749
[5] R. Anderson and D. M. Bevly, "Estimation of tire cornering stiffness using GPS to improve model based estimation of vehicle states", *Proceedings of the IEEE Intelligent Vehicles Symposium*, 2005, p 801-806
[6] H. E. Tseng, "Dynamic estimation of road bank angle", *Vehicle System Dynamics*, vol. 36, no. 4-5, 2001, pp. 307-328
[7] L. R. Ray, "Nonlinear State and Tire Force Estimation for Advanced Vehicle Control", *IEEE Transactions on Control Systems Technology*, vol. 3, no. 1, 1999, pp 117-124
[8] L. Imsland, T. A. Johansen, T. I. Fossen, J. C. Kalkkuhl, and A. Suissa, "Nonlinear observer for vehicle velocity estimation", *SAE International 2006*

[9] A. von Vietinghoff, M. Hiemer, and U. Kiencke, "Nonlinear observer design for lateral vehicle dynamics", *IFAC World Congress 2005*

[10] U. Kiencke and A. Daiss, "Estimation of Tyre Friction for Enhaced ABS-Systems", *Proceedings of the AVEG'94*, 1994

[11] M. Lakehal-ayat, H. E. Tseng, Y. Mao and J. Karidas, "Disturbance Observer for Lateral Velocity Estimation", *Proceedings of AVEC, 8th International Symposium on Advanced Vehicle Control*, 2006

[12] S. Van Huffel and J. Vandewalle, "The Total Least Squares Problems: Computational Aspects and Analysis", Frontiers in Applied Mathematics, *SIAM Philadelphia*, 1991

[13] L. Ljung and T. Söderström, "Theory and Practice of Recursive Identification", *MIT Press*, Cambridge, Massachusetts, USA, 1983